International Journal of Pharmaceutics 370 (2009) 8–16

Contents lists available at ScienceDirect

International Journal of Pharmaceutics

journal homepage: www.elsevier.com/locate/ijpharm

Terahertz pulsed imaging and near infrared imaging to monitor the coating process of pharmaceutical tablets

Lene Maurer[a,b,*], Hans Leuenberger[b,c,d]

[a] F. Hoffmann-La Roche Ltd., Grenzacherstrasse, 4070 Basel, Switzerland
[b] Institute of Pharmaceutical Technology, University of Basel, Klingelbergstrasse 50, 4056 Basel, Switzerland
[c] Institute for innovation in industrial pharmacy Ifiip llc, P.O. Box, 4011 Basel, Switzerland
[d] Department of Pharmaceutics and Biopharmaceutics, School of Pharmaceutical Sciences, University of Geneva, University of Lausanne, 30 Quai Ernest-Ansermet, 1211 Geneva 4, Switzerland

ARTICLE INFO

Article history:
Received 14 April 2008
Received in revised form 4 November 2008
Accepted 10 November 2008
Available online 25 November 2008

Keywords:
Near infrared (NIR) imaging
Terahertz pulsed imaging (TPI)
Pharmaceutical
Tablet
Coating

ABSTRACT

Terahertz pulsed imaging (TPI) and near infrared (NIR) imaging were used to non-destructively monitor the coating process of film-coated tablets. Samples that were taken from a pan coater at different time points were analyzed by both methods. TPI provided coating thickness maps over the whole surface of the tablets, determining the thickness of the coating at each point of the sample surface in μm, this way also giving information about the coating uniformity. The growth of the coating during the coating process was shown. NIR imaging did not provide direct thickness values, but by different absorbance values, inter- and intra-tablet differences were shown. Thus, coating thickness information was also obtained in a way that different tablets could be compared. The growth of the coating layer during the process was shown as well. Both methods provided comparable results; and they were able to detect small defects in the coating. With TPI, the whole tablet surface could be scanned; with NIR imaging information about the tablet ends at the center-band was not obtained due to the strong curvature. NIR imaging proved to be better at thinner coating layers and had a higher spatial resolution whereas TPI had the clear advantage that it provided direct thickness values.

1. Introduction

Tablets are the most common pharmaceutical dosage forms. Often, they are film-coated due to various reasons. A coat can for example improve the shelf-life of the product by protecting the tablet core against moisture or light, this way preventing the degradation of the active pharmaceutical ingredient (API). A coat can also serve for determining the appearance of the product and making it easier for the patient to recognize a tablet by a specific color. It can mask an unpleasant taste or odor and make it easier to swallow. As the coat acts as a barrier between a core that contains high-potent API and the environment, it allows the manufacturer to handle the coated product like a normal product without special precautions that are necessary for high-potent products. Important fields are coatings that modify or control the drug dissolution rate. For example coatings that show pH-dependent behavior allow the disintegration of the tablet only in the small intestine but not in the stomach; or they control the release of the API by a limited diffusion of the API through the coating layer. The coating thickness and uniformity are important, as they are closely related to its functionality. A wrong coating thickness may have unwanted effects: for example, if it is too thick, the dissolution may be too slow, if it is too thin, it might not protect the core sufficiently against humidity. But not only the average coating thickness is important, also the uniformity: the coat can only be as good as its weakest point, for example its thinnest spot. This clearly explains that the quality of the film coat has to be controlled. But not only the quality of the final product is of interest. In order to have a robust coating process, the process has to be understood. This process understanding/knowledge is an important point of the Process Analytical Technology (PAT) initiative of the FDA (FDA, 2004). One step to understand the coating process better is to monitor it.

There are various methods to analyze the coating and the coating process of tablets. One can for example weigh the vessel from which the coating solution is taken during the coating process continuously or calculate the amount of applied coating mass from the flow- or spray-rate of the coating liquid. Both methods are indirect and give only average information. A classical method to monitor the coating process is to take samples during the process, weigh a known sample size and compare the weight of the samples with coat with the weight of the same amount of uncoated samples. This

* Corresponding author at: F. Hoffmann-La Roche Ltd., Grenzacherstrasse, 4070 Basel, Switzerland. Tel.: +41 61 688 6728; fax: +41 61 688 5103.
E-mail address: lene.maurer@roche.com (L. Maurer).

0378-5173/$ – see front matter © 2008 Elsevier B.V. All rights reserved.
doi:10.1016/j.ijpharm.2008.11.011

allows determining the theoretical amount of applied coating mass. Again, this method is indirect and does not give information about coating uniformity. Another problem with this method is that the mass loss of core material during the process due to friability is not taken into account. Also, loss on drying differences between core and film-coated tablet may influence the results. A better evaluation of the film coat thickness and uniformity might be obtained through functionality testing by disintegration or dissolution studies, but those tests are destructive, indirect, time-consuming and laborious measurements. Another destructive method is optical microscopy that provides direct thickness data. For coating uniformity determination it is only partly suited as the coating thickness is measured only at a few points and not over the whole tablet surface. Other methods to analyze the coating of tablets include scanning electron microscopy, attenuated total reflection–infrared (ATR-IR) imaging (Reich, 2002), confocal laser scanning microscopy (Ruotsalainen et al., 2003), laser induced breakdown spectroscopy (LIBS) (Mowery et al., 2002), Raman spectroscopy (Romero-Torres et al., 2005; El-Hagrasy et al., 2006; Kauffman et al., 2007) and near infrared (NIR) spectroscopy (Kirsch and Drennen, 1995, 1996; Andersson et al., 1999; Pérez-Ramos et al., 2005; Roggo et al., 2005). Most of the techniques have disadvantages such as being destructive, indirect and laborious measurements that provide only average data.

In the presented study, two imaging methods were used to analyze the coating and monitor the coating process of tablets. Imaging methods have the advantage that they do not only give one average result per sample, but spectra or values are obtained from many spots of the sample. Moreover, both methods were fast and non-destructive.

The first method was terahertz pulsed imaging (TPI). It is a relatively new method that can be used to analyze coating thickness of tablets. The terahertz (THz), also called far-infrared, region is located between the mid-infrared and microwave region of the electromagnetic spectrum. It covers the range from 30 to 3000 μm, or 100 GHz to 10 THz. Terahertz radiation can induce intermolecular bond vibrations, large-mass intramolecular oscillations and phonon lattice dynamics (Walther et al., 2003; Day et al., 2006). All those interactions are strongly distinct in crystalline materials but not in amorphous materials. As many materials used in pharmaceutics e.g. lots of excipients and most tablet coating materials are amorphous, they have low terahertz absorptivity and are semitransparent in the terahertz region. Compared to other spectroscopic techniques such as Raman or infrared, this allows a deep probing of the sample (Zeitler et al., 2006). Due to the low energy nature of the terahertz radiation, there is no danger to heat the material or to induce photochemical reactions. In TPI, the terahertz pulse is generated by an ultrashort laser pulse on a so-called terahertz emitter. The resulting short pulses of coherent THz radiation interact with the sample and are detected by the so-called terahertz receiver. The technique is time-resolved and the time the THz pulse needs can be measured. The obtained time domain spectrum directly provides information about the internal structure of the sample. This is due to the fact that the coherent terahertz pulse is reflected by internal layers of the sample, e.g. different coating layers in a tablet. Wherever there is sufficient change in the refractive index, a part of the pulse is reflected from this interface. The time delay of the reflected pulses depends on the depth of the feature, therefore the thickness of a coating or the depth of the feature can be calculated by the time delay. This means that the exact composition of the core of a tablet, for example, is secondary. In TPI, a terahertz time-domain signal is taken at many points mapped over the surface of a sample. Those multiple point measurements are used to build a coating thickness map over the sample surface by calculating the thickness from the time delay at each point. Thus TPI provides three-dimensional information: the *x*- and *y*-axis describe vertical and horizontal dimensions of the sample and the *z*-axis represents the time-delay, i.e. depth, dimension. Due to the coherent nature of the signal, the technique has a very high signal-to-noise ratio, and it can be applied at room-temperature. As the macroscopic structures on the surface of tablet samples are much smaller than the wavelength, scattering is not significant (Wallace et al., 2004). The lateral resolution is limited by the wavelength and the depth resolution is limited by the pulse duration. In a pharmaceutical context, it has been mainly used for the analysis of coating thickness and uniformity of tablets (Fitzgerald et al., 2005; Zeitler et al., 2006; Ho et al., 2007). Analysis of soft gelatine capsules layer thickness by TPI was also reported (Zeitler et al., 2006). Coating thickness results have been correlated with the dissolution of delayed release tablets (Spencer et al., 2007) and recently, a study compared terahertz pulsed imaging coating thickness determination with near infrared spectroscopy results (Cogdill et al., 2007). In the presented paper, TPI was investigated for its ability to monitor the coating process of film-coated tablets. For a first feasibility study, tablets of one product with different coating thicknesses were analyzed. A tablet of another product was used to determine the ability of the technique to detect fine structures. Samples that were taken out of the coater during the coating process were used for the monitoring study. The focus lay on coating thickness analysis and the analytical method. This meant that, as explained above, detailed information about the exact composition of the tablet cores were not necessary and therefore of no importance for the study. For this reason and also for trade secrecy, detailed information about the cores is not given. The same applies for the used pan coaters: only the tablet coating layer was analyzed, and the performance of the coaters were not under investigation in this study. Details about the used coaters are therefore not given.

The TPI results of the monitoring of the coating process were compared with NIR imaging analysis. Advantages and disadvantages as well as limits of both techniques are discussed. In near infrared imaging, not only one spectrum is obtained like in classical spectroscopy, but several thousand spectra. The near infrared region covers the range from 800 to 2500 nm of the electromagnetic spectrum. NIR absorbances are overtone and combination bands from the fundamental mid infrared absorbances. The spectra provide for example information about the chemical identity and the spatial data provide information about the distribution. Several applications of NIR imaging in pharmaceuticals have been reported. For example, it was used to determine powder blend homogeneity (El-Hagrasy et al., 2001) and blend uniformity in final dosage products (Lyon et al., 2002). It also served for the identification of tablets in blister packs (Malik et al., 2001) and to extract process related information from tablets and pre-tabletting blends (Clarke, 2004). Recently, it was used for content uniformity determination of tablets (Gendrin et al., 2007). It was also applied for the examination of the internal structure of time-release granules (Lewis et al., 2001), but coating analysis by NIR imaging is not widespread.

2. Material and methods

2.1. Samples

Three different products—products A, B, and C, respectively—were analyzed. All products were coated in pan coaters in medium or large scale. 16 tablets of product A were used for a first evaluation of TPI. The tablets contained 36% of active pharmaceutical ingredient (API) with lactose and cellulose as main excipients. They were produced via a wet granulation step. The tablets were coated with Opadry White and only tablets with finished coating were analyzed. On the first part, batch a, the coating weight was 3% of the core weight. Those samples were named Aa1, Aa2, etc. On the second part, batch b, the coating weighed 5% of the core

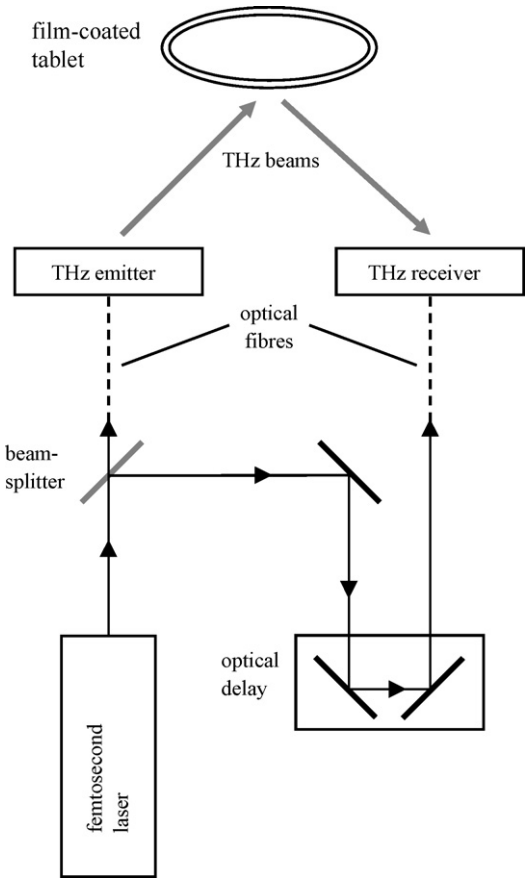

Fig. 1. Schematic setup of the TPI imaga 2000 system.

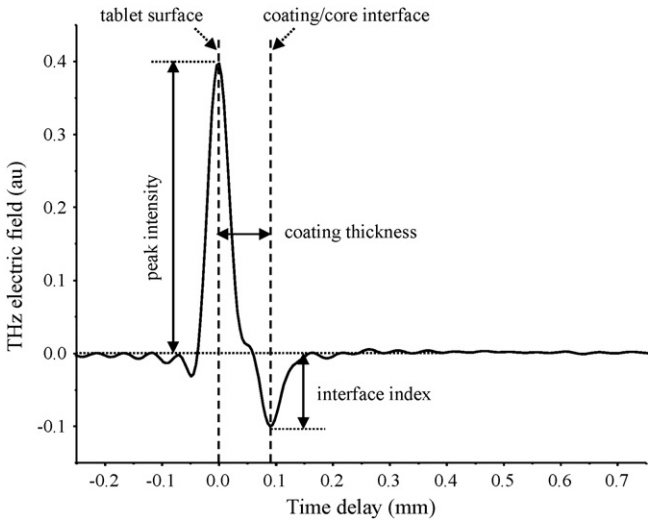

Fig. 2. Typical terahertz waveform. Reflection from the tablet surface (i.e. air/coating interface) and from the coating/core interface are indicated by dashed lines; drawn through arrows indicate how TPI parameters (peak intensity, interface index, layer thickness) are related to the waveform.

weight; samples were named Ab1, Ab2, etc. Product B was analyzed by TPI and NIR imaging. The tablets contained 78% of API and lactose as main excipient. They were produced via a wet granulation. The tablets were coated with Opadry Pink and they were embossed on both faces. Tablets were taken out of the coating pan during the coating process at different time points in order to monitor the coating process and to demonstrate the correlation between signal and coating thickness. 20 samples were analyzed, they were named B1–B20, B1 having been sampled at the beginning of the process and with hardly no coating, and B20 at the end, thus having the thickest coating. Additionally, one uncoated tablet core of product B, tablet B0, was used as reference tablet for NIR imaging. Tablets of the same batch were used to demonstrate the growth of the coating by weighing. 10 tablets were taken at each sampling time point and weighed, the mean tablet weight was then used. Product C, also featuring an embossing, contained 62% of API. It was produced via hot-melt extrusion and it was coated with Opadry Yellow. A sample was stressed during storage to develop cracks in the coating. The sample was named C and used for an evaluation of the ability of TPI to detect fine cracks. The upper face (face a), lower face (face b) and the center-band of each tablet were analyzed.

2.2. Terahertz pulsed imaging

For analysis of the coating thickness and uniformity of all three products, a TPI imaga 2000 with acquisition software TPIScan and data analysis software TPIView (all TeraView Ltd., Cambridge, UK) was used. Fig. 1 shows the schematic diagram of the instrument. A Ti:Sapphire femtosecond laser at 800 nm and THz emitter and receiver are used for generation and detection of terahertz pulses. The sample is hold by a suction cup on a robotic arm. This robotic arm moves the tablet in front of the static emitter/receiver probe head and thus allows the scanning of the sample surface. On multiple points of the sample surface, measurements are made, resulting in a mapping of the sample surface and thus providing coating thickness information. Each point, or pixel, has the size of 200 μm × 200 μm. Depending on the size of the sample, more or less point scans can be recorded. For product A, 2000 point measurements were recorded over both faces of each tablet as well as the center-band. For product B, 3200 point scans were recorded on each face and 2800 points were measured on the center-band. The number of point scans for product C was 5300. Measurement time was 20–30 min per tablet. Reference measurements were made on a metallic mirror.

Fig. 2 shows a typical terahertz waveform of one point measurement. Whenever a reflection of the pulse at an interface occurs, the waveform shows a peak. A change from a lower to a higher refractive index results in a positive peak; if the refractive index gets smaller, a negative peak occurs. In Fig. 2, the high, positive peak indicates the reflection of the pulse at the tablet surface, i.e. air/coating interface. The second peak, which is smaller and negative, results from the reflection at the coating/core interface. Several informations can be extracted from this waveform. From the time delay between the maximum of the first peak and the minimum of the second peak, the thickness of the coating can be calculated. As the peak intensity of the air/tablet surface depends on the refractive index of the tablet surface and as it can be affected for example by the roughness of the surface, it can provide information about the smoothness of the surface. The interface index, which is the peak height ratio of the reflection from the coating/core interface and the reflection from a metallic mirror (the reference measurement), provides information about the coating/core interaction. As such a waveform is obtained at each measured point, providing the named information at each point, maps displaying the different characteristics can be built, for example coating thickness maps. A coating thickness map shows the coating thickness at each point of the surface of the sample, this way also providing information about coating uniformity.

The measurements resulted in coating thickness maps and histograms for all products, providing information about the thickness as well as uniformity of the coating. For product C, also a peak intensity map and an interface index map were built to detect small defects in the coating layer.

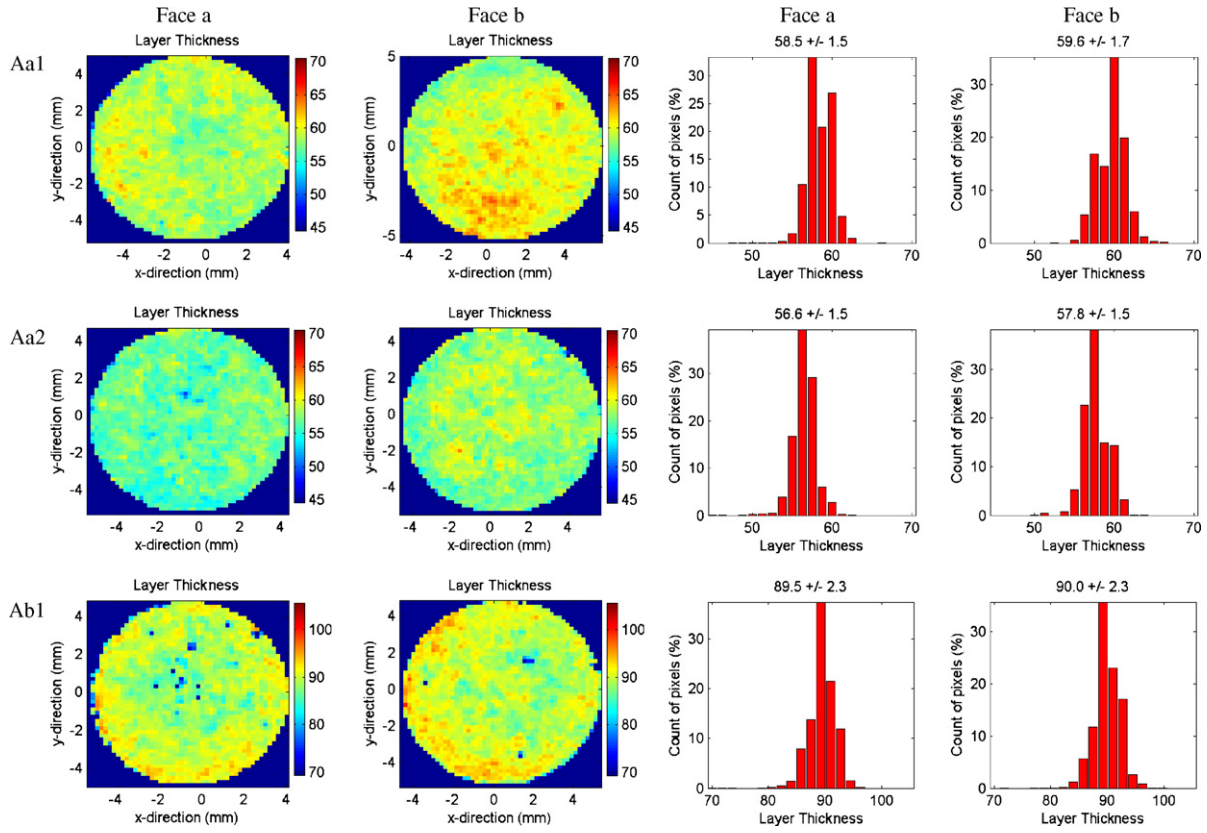

Fig. 3. Coating thickness maps and histograms of tablets Aa1, Aa2, and Ab1. Note that the color scale for tablet Ab1 is different from the ones of tablets Aa1 and Aa2. Differences between the two batches, tablets, tablet faces, and within individual faces can be observed. (For interpretation of the references to color in this figure legend, the reader is referred to the web version of the article.)

2.3. Near infrared imaging

For acquisition of NIR images, the Sapphire with SapphireGo software (Malvern instruments Ltd., Malvern, UK) was used. The instrument is equipped with a focal plane array (FPA) detector of a size of 256 × 320 pixels which allows the acquisition of 81920 spectra simultaneously. Spectral range covered 1100–2450 nm with a spectral resolution of 10 nm; each image was collected as 16 coadds. Each pixel was 80 μm × 80 μm. Both faces of each tablet were imaged as well as the two flat sides of the center-band. Due to the strong curvature of the round parts of the center-band and resulting focus problems, imaging was not possible at those parts. Measurement time was below 5 min for each image, thus below 20 min for the 4 images obtained per sample. An image of Opadry Pink powder was taken for reference. Data were treated using ISys software (Malvern instruments Ltd., Malvern, UK). From all images, bad pixels were removed by applying a 3 × 3 median filter and spectra were converted to absorbance units. The areas on the images that were around the tablets were removed by masking. Standard normal variate (SNV) transformation was performed. Mean spectra of tablet B0, tablet B20, and Opadry Pink were computed for comparison. The images were then used as this or a Savitzky–Golay second derivative was applied. Images were either analyzed individually or several images were concatenated to form a bigger image which was then analyzed. On the images of the tablets, different methods were tried. The images were examined at single wavelengths that are characteristic for core or coating. Principal component analysis (PCA) was performed as well as partial least squares (PLS) discriminant analysis. For PLS, mean spectra of the core and of the longest coated tablet were used as reference.

3. Results and discussion

3.1. Terahertz pulsed imaging

3.1.1. Product A

Measurements gave an average coating thickness of 56.5 μm for tablets of batch a and 76.5 μm for tablets of batch b; the minimum was 53.0 μm and the maximum was 92.5 μm. TPI clearly detected the inter-batch differences that could be expected from the fact that more coating mass was applied on batch b. Intra-batch differences and differences on individual tablets were also detected. Fig. 3 shows the coating thickness maps and histograms of tablets Aa1 and Aa2, and Ab1. Both sides (face a and face b) are shown. Intra-batch differences can be seen by comparing the images and histograms of tablets Aa1 and Aa2; tablet Aa1 has a slightly thicker coating. Differences of coating thickness on individual faces can also be observed, e.g. on face a of tablet Ab1, where the coating in the center seems to be slightly thinner than at the edge. As can be seen on the images of tablet Aa2, there can also be differences of coating thickness between the two faces of one tablet. Face a has a thinner coating than face b. However, the differences are small and none of the tablets displayed real defects in the coating.

3.1.2. Product B

On tablet B20, a precision study was undertaken. Ten repeat measurements were recorded over 4 days (three measurements on the first three days each and one measurement on day 4), determining the coating thickness on both faces and the center-band. Mean thickness over the ten repeats was 58.25 μm with a standard deviation of 0.21 μm for face a, 52.21 μm with a standard deviation of 0.19 μm for face b, and 44.8 μm with a standard devia-

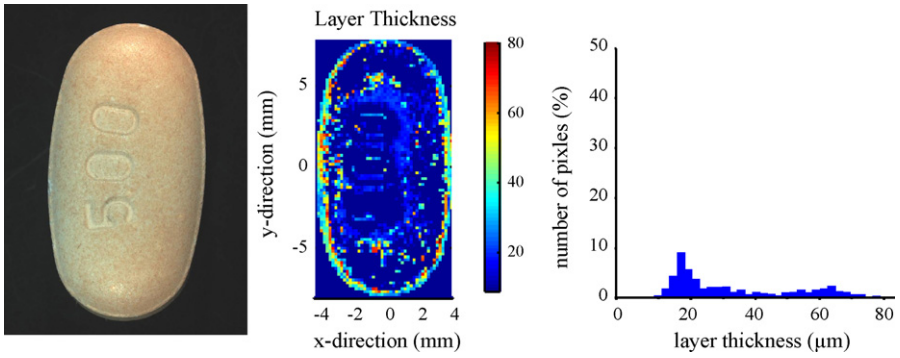

Fig. 4. Photograph, coating thickness map and histogram of tablet B1. Sample taken at the beginning of the coating process. Photograph shows the beginning coating layer, histogram indicates that layer thickness is below the detection limit of the instrument.

tion of 1.03 μm for the center-band, thus demonstrating very good repeatability. The higher standard deviation at the center-band compared to faces a and b is due to the instrument scanning close to and around the edges of the center-band. The coating thickness of tablet B1 could not be determined by TPI because the thickness was below the detection limit of the instrument. This can be seen in Fig. 4, where the visible image, coating thickness map and histogram of face a are shown. The start of a coating layer can be seen in the photograph as little reddish dots on the tablet, but as the coating is very thin the core is still clearly visible, what was expected due to the fact that the sample was taken at the beginning of the coating process. The very broad distribution in the histogram indicates that a coating thickness measurement by TPI is not possible at this point of the coating process. However, this does not pose a problem, as coating layers on tablets from a later stage of the process and on finished products are much thicker and do normally not lay under the detection limit of the instrument. Table 1 shows the average coating thickness of tablets B2–B20 for both sides and center-band, including the standard deviations. Average coating thickness ranges between 22.5 and 58.5 μm. Fig. 5 plots the data from Table 1, showing the growth of the coating thickness against time. The coating on the center-bands tends to be thinner than on the top and bottom faces. This might be explained by the fact that in a pan coater, the top and bottom sides of a tablet have a higher probability to face the spray nozzles than the center-band. Fig. 6 shows the coating thickness maps of face a of all 20 tablets. Defects in the coating can be observed: for example, tablet B14 shows a defect close to the "5" of the embossing on face a. This is a scratch that occurred during sample handling and which removed the coating layer on that area. It can also be observed that on all tablets, the coating at the embossing seems to be thinner than on the rest of the tablet. This is unlikely. It is assumed that this is an artifact of the measurement. The spatial resolution is 200 μm × 200 μm, but the width of the embossing fonts of product B is slightly smaller. Therefore at the embossing, the focus of the THz pulse that is crucial for correct measurement can not be guaranteed, probably resulting in wrong thickness indications. To support the TPI results of the coating growth, the weight gain of the tablets during the coating process is shown in Fig. 7.

3.1.3. *Product C*

Due to the fact that the determination of the coating thickness at the embossing of product B seemed to be problematic, the question arose if fine structures such as thin cracks can be detected by the instrument or not. As can be seen on the photograph in Fig. 8, tablet C has fine cracks in the coating in the region of the embossing. The picture was taken under a microscope with approximately 6× magnification. In the coating thickness map, also shown in Fig. 8, these cracks cannot be seen. However, on the peak intensity map and especially on the interface index map (see also Fig. 8), features corresponding to the cracks on the visible image can be seen. Although the cracks are not shown on the coating thickness map, the instrument detected a failure at the area of the cracks and displayed it on the peak intensity map and on the interface index map. This shows that fine features are a problem with coating thickness

Table 1
Average coating thickness with absolute standard deviations of tablets B2–B20. All values in μm.

Sample	Average coating thickness of face a	Standard deviation (of average coating thickness of face a)	Average coating thickness of face b	Standard deviation (of average coating thickness of face b)	Average coating thickness of center-band	Standard deviation (of av. coating thickness of center-band)
B2	24.0	7.8	23.0	6.1	23.8	5.8
B3	22.5	4.9	24.2	6.3	22.6	7.1
B4	27.4	7.0	25.8	5.5	23.3	7.0
B5	27.7	3.8	25.2	5.0	24.5	6.8
B6	32.4	4.7	38.3	5.4	29.7	6.0
B7	25.0	5.1	24.3	6.2	23.1	4.7
B8	26.7	5.1	26.7	5.5	25.4	4.7
B9	29.9	5.1	32.1	5.1	26.0	3.9
B10	40.7	5.8	34.7	5.4	29.9	4.6
B11	30.2	5.3	29.1	5.5	26.5	5.9
B12	29.7	5.1	27.4	6.2	25.9	4.9
B13	32.9	6.0	40.2	5.3	30.1	3.5
B14	28.8	5.5	29.2	5.8	26.5	3.9
B15	51.9	4.8	52.5	4.9	39.9	4.3
B16	45.9	4.7	49.2	4.6	38.9	4.0
B17	43.1	4.7	39.5	4.6	32.2	4.1
B18	41.7	5.0	39.3	5.2	35.0	3.7
B19	42.3	4.6	43.1	5.0	38.9	4.0
B20	58.5	4.6	52.1	4.7	44.2	3.8

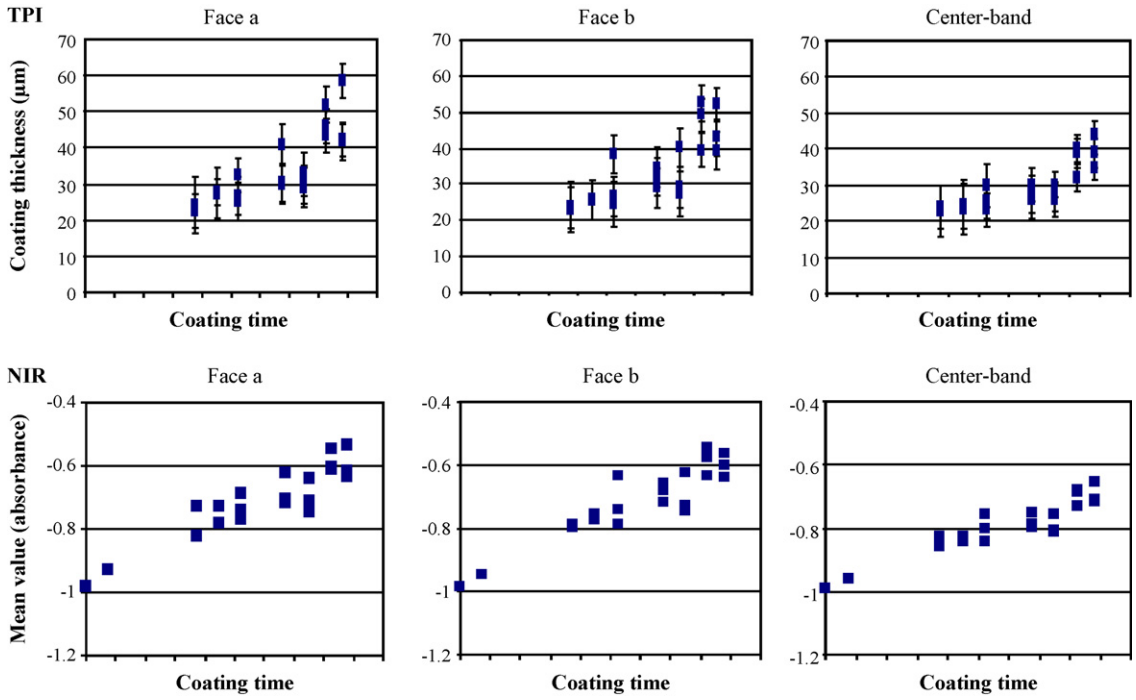

Fig. 5. (Top) Plot of the data from Table 1, showing the growth of the coating thickness against time. Error bars display the standard deviation for each measurement. (Bottom) Mean near infrared values of absorbance at 1390 nm of tablets B0–B20 plotted against coating time. Increasing absorbance values indicate growth of the coating layer during the process.

maps, although by consideration of the other information that the waveform provides, it might be possible to detect small defects nevertheless. However, the cracks in the coating were still easily visible on a photograph with approximately 6× magnification. A coating might have even finer cracks, so-called hairline cracks. Surely those small defects will not be detected by building a coating thickness map, and it is in question if defects of such a small size can be detected by peak intensity or interface index maps.

3.2. Near infrared imaging

Fig. 9 shows the mean near infrared spectra of Opadry Pink, tablet core and the longest coated tablet. One can see peaks in the core spectrum that are not visible or much weaker in the coated tablet spectrum and vice versa. Comparison with the Opadry Pink spectrum explains that those differences are due to the coating material. For example, a characteristic peak of Opadry Pink lies at 1390 nm. A peak at this wavelength is also visible in the coated tablet spectrum, but not in the core spectrum, indicating that a differentiation between coated and uncoated tablets should be possible at this wavelength. In the core spectrum, peaks are for example distinctive at 1460, 2060 and 2120 nm. They are also present in the coated tablet spectrum, but less strong, thus providing possibility to differentiate between coated and uncoated tablets at those wavelengths. Images of face a of tablets B0, B1, B2, B6, B9, and B18 were concatenated and looked at the different wavelengths that showed to be characteristic for core and coated tablet, respectively. The best wavelengths for differentiating between coated and uncoated tablets as well as for visualization of the growth of the coating during the process proved to be 1390 and 2120 nm. Fig. 10 shows those two images as well as the mean spectra of the six tablets at the region of the two specific wavelengths. The absorbance at 1390 nm increases from the uncoated sample on the left to the most coated tablet on the right, visualizing the growth of the coating in the image by showing higher intensity values on the right. This could be expected as 1390 nm is a characteristic wavelength for Opadry Pink, the coating material. The coating thickness growth results in an increase in the absorbance. At 2120 nm, this is exactly the other way round. The visualization of the growth of the coating layer was also possible by using Savitzky–Golay second derivative or by applying PCA and PLS, but no additional information was gained by those methods.

In the concatenated image, a good and easy comparison between the different tablets is possible as all images are scaled to the same intensity color scale. However, due to computational power limits, it was not possible to concatenate the images of all tablets. Therefore, single images were used in order to analyze all tablets. Images at 1390 nm of face a of tablets B1–B20 are shown in Fig. 6. The increase in the coating thickness from uncoated to fully coated tablets is not as easily visible as in the concatenated image. As each image has its own color scale, an inter-tablet comparison is more difficult than in the concatenated image. But the intra-tablet differences are better seen in the single images. However, a comparison between the tablets is also possible by considering the different color scales. Absorbance values, indicated by the intensity color scale, increase from the image of tablet B1 to the image of tablet B20. This can be seen in Fig. 5, where the mean values of the single images of tablets B0–B20 are plotted against the coating time. The absorbance of the samples over the coating process increases, this way indicating the growth of the coating.

Results from face b are equivalent. The situation at the center-band is more difficult. Not the whole center-band could be imaged due to focus problems at the strongly round ends of the tablets. Only the imaging of the flat side of the center-band was possible. However, similar calculations as on faces a and b, respectively, were possible and resulted in similar data, but it must be kept in mind that not all the center-band is looked at. Overall, the absorbance values at the center band were lower than at the faces, indicating a thinner coating layer at the center-band.

3.3. Comparison of TPI and NIR imaging

Fig. 6 shows the coating thickness maps of face a of tablets B1–B20 and the near infrared images of face a of the same tablets

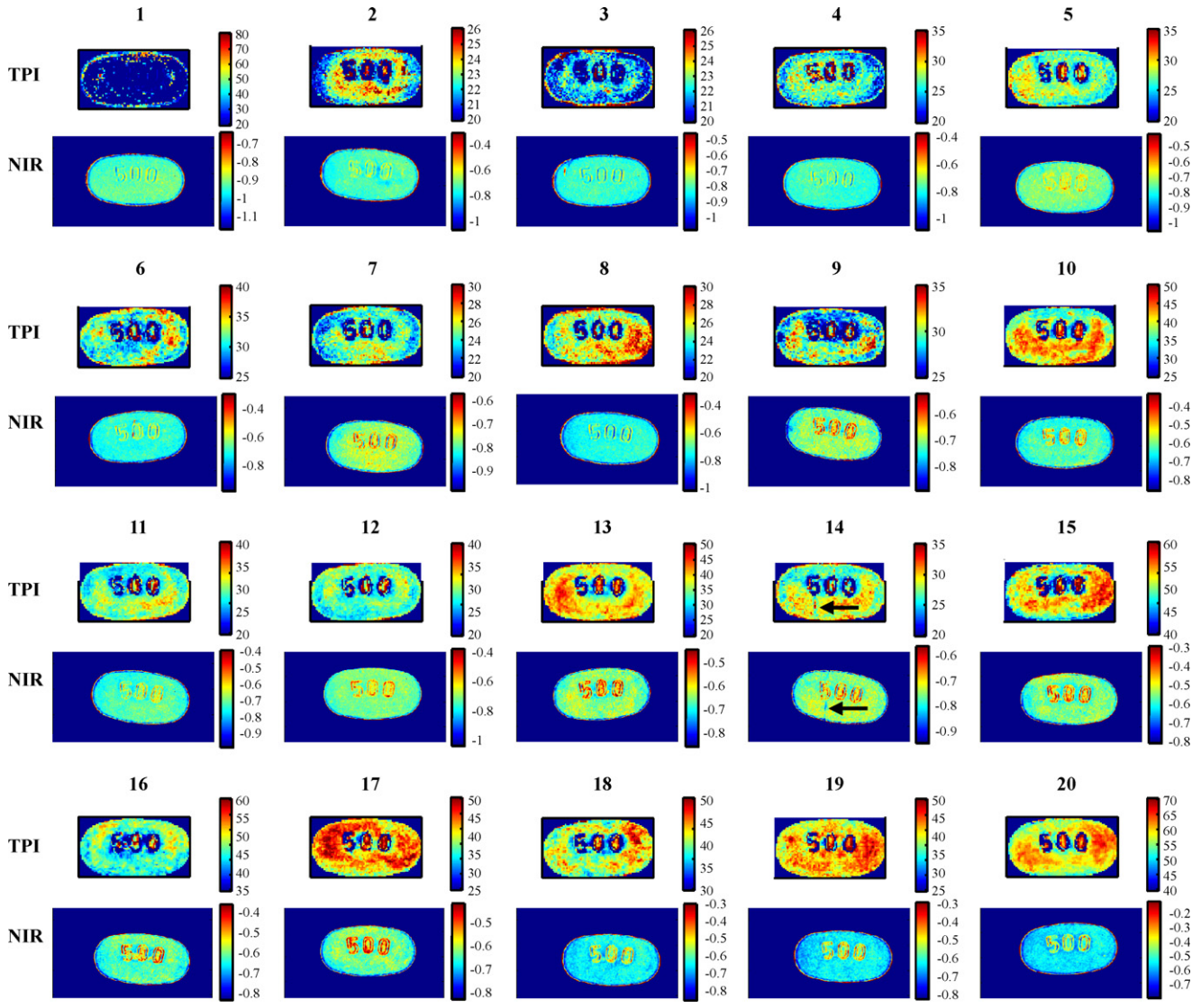

Fig. 6. TPI coating thickness maps and NIR images at 1390 nm of face a of tablets B1–B20. Color scales of the coating thickness maps indicate thickness in μm; color scales of NIR images give absorbance values. TPI and NIR images show the same pattern of coating layer distribution. Defects can be determined, for example a scratch on tablet 14 (indicated by arrows). (For interpretation of the references to color in this figure legend, the reader is referred to the web version of the article.)

at 1390 nm. Each image has its own color scale, i.e. the lowest value in the image is the lowest value of the color scale and the highest value is the highest, respectively. This accentuates the intra-tablet differences. Comparing the TPI image and the NIR image of one tablet, it can be seen that they both have the same pattern. Where the TPI coating thickness map indicates a thicker coating layer, the absorbance in the NIR image is higher as well. Defects in the coat are also visible in images of both techniques. For example, the scratch in the coating layer of tablet B14 is detected in the TPI map as well as in the NIR image. The biggest differences between each pair of images

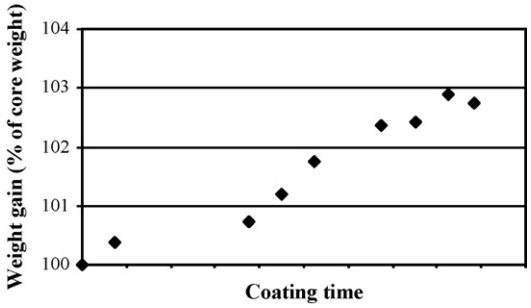

Fig. 7. Weight gain of tablets of product B during the coating process. Weight gain of the mean weight of 10 tablets at each time point is shown.

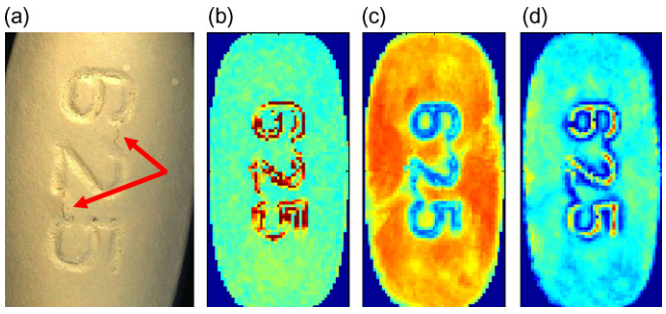

Fig. 8. Tablet C: (a) Photograph with 6× magnification, cracks in the coating indicated by arrows; (b) coating thickness map; (c) peak intensity map; (d) interface index map. Cracks are not visible in the coating thickness map but can be seen in the peak intensity map and the interface index map.

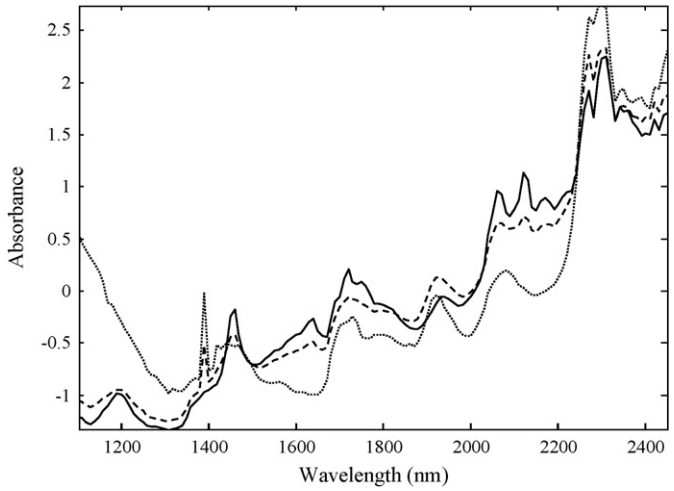

Fig. 9. Mean NIR spectra of tablet core (solid line), longest coated tablet (dashed line) and Opadry Pink (dotted line), displaying characteristic peaks. Differences between the core and the coated tablet due to Opadry Pink are visible due to different absorbance values for example at 1390, 1460, 2060, and 2120 nm.

lies at the embossing. The NIR images show higher absorbance at the embossing, thus indicating a thicker coating layer, whereas the TPI coating thickness maps show a lower coating thickness at those parts. As discussed, the determination of coating thickness at the embossing of this product by TPI is problematic and the coating thickness values given there are considered as an artifact of the measurement. The NIR images have a higher spatial resolution than the TPI maps and therefore allow a more accurate analysis at problematic regions like the embossing. Another difference is the fact that at the NIR images, the coating at the edge of the tablet seems to be thicker than at the rest of the face. This is not visible in TPI coating thickness maps. As in TPI the surface is mapped point by point, such edge effects can be avoided for example by not considering the outermost ring of point measurements. In NIR imaging with a FPA, where the whole sample is imaged at once, edge effects can be a problem. In this case, it might be due to the fact that the center-band is located "below" the edge of the face, this way imitating a thicker coating layer. But as it is the same for each tablet, the influence when comparing them should not be too big. An advantage of NIR imaging is the lower detection limit. With TPI, the coating thickness of tablet B1 could not be determined because it was below the detection limit of the instrument. With NIR imaging, detection is possible, a clear difference between tablet B1 and the uncoated tablet B0 can be seen. On the other hand, it can be expected that when the coating gets very thick, TPI will still be able to determine the layer thickness whereas with NIR imaging, this might not be possible. When the coating has reached a certain thickness, NIR radiation will not reach the core anymore, therefore only information about the coating will be contained in the spectra. Then, it does not matter if the coating gets even thicker as differentiation is not possible any more. Another advantage of TPI is the fact that the whole center-band can be analyzed. In NIR imaging, this was not possible due to the very strong curvature of the ends of the tablet. From a measurement time point of view, the differences are not too high if the full spectrum is used in NIR imaging. If only a few wavelengths are looked at, acquisition time decreases considerably and NIR imaging becomes much faster. The biggest advantage of TPI is surely that it is a direct measurement and coating thickness values are obtained directly. NIR imaging is an indirect method, not the thickness is measured but the change in absorption at a certain wavelength. This allows good intra- and

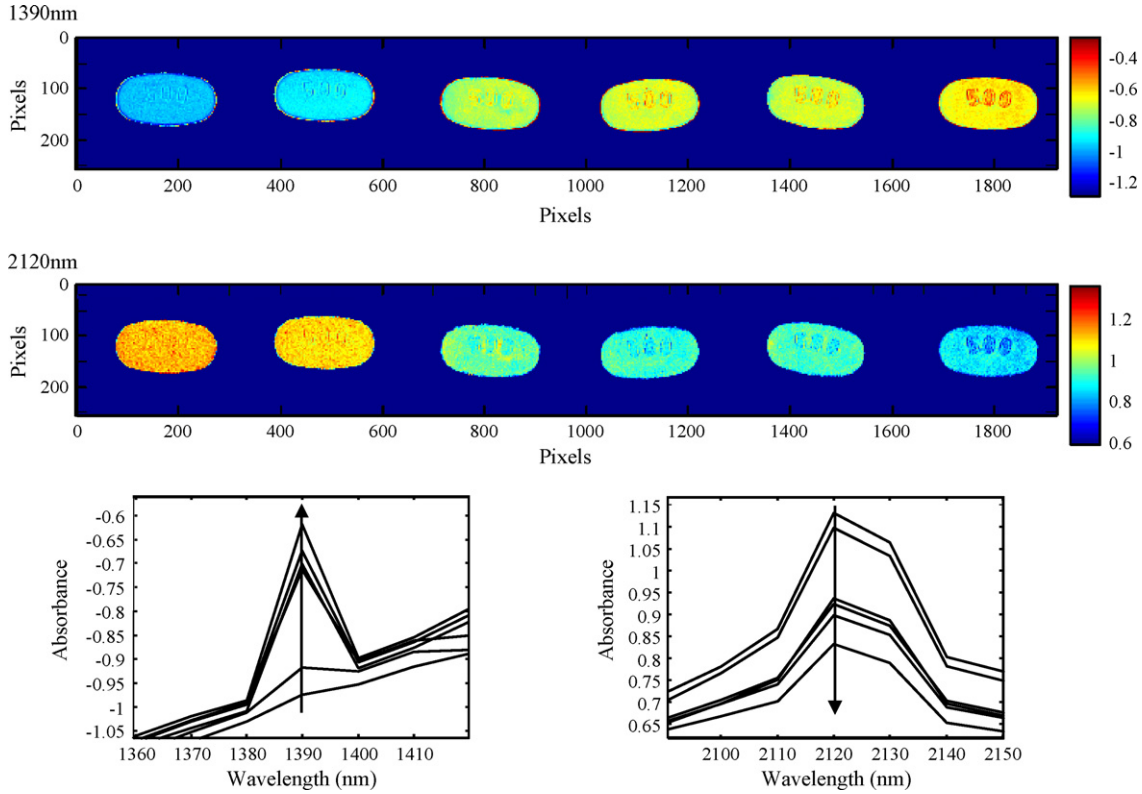

Fig. 10. (Top) Concatenated NIR image of tablets B0, B1, B2, B6, B9, B18 (from left to right) at 1390 and 2120 nm, showing the growth of the coating layer by change in absorbance. Color scale indicates absorbance values, with red being the highest and blue being the lowest absorbance, respectively. (Bottom) Parts of the mean NIR spectra of tablets shown in the concatenated image, arrow indicating the growth of the coating layer. (For interpretation of the references to color in this figure legend, the reader is referred to the web version of the article.)

inter-tablet comparison but in order to know how thick the coating layer actually is, other methods like TPI have to be applied and a calibration has to be made. It has also to be considered that in NIR imaging, as changes in absorption values are used, the spectra of coated and uncoated tablets have to be different enough to extract the wanted information. In this study, it was easily possible at a single wavelength, but it might be more difficult with other products. One other advantage of TPI is the low energy nature of the used THz radiation, this way not heating the sample. Depending on the measurement time and the temperature sensitivity of the samples, heating might be a problem in NIR imaging where the radiation is much more energetic. The two methods have in common that they are non-destructive, a sure advantage over other methods such as LIBS or optical microscopy where the sample has to be sectioned. When comparing the average thickness values given by TPI with the mean absorbance values of the NIR images (Fig. 5), both methods show the growth of the coating layer during the process. Both methods do also detect a thinner coating layer at the center-band compared to the faces of the tablets. This is probably due to the fact that the tablets in the pan coater have a higher probability to face the spray nozzles with the relatively flat sides rather than with the center-band.

4. Conclusion and outlook

TPI and NIR imaging were used for the monitoring of the coating process of film coated tablets. Both fast, non-destructive methods were able to visualize the growth of the coating layer. TPI measurements provided direct coating thickness values over the whole sample surface, this way also showing inter- and intra-tablet differences. NIR imaging also gave information about inter- and intra-tablet coating layer differences, but as an indirect method, real layer thickness values were not obtained. The pattern of the coating thickness distribution as shown by TPI coating thickness maps and NIR images is the same. The spatial resolution of NIR is better than that of TPI, and NIR imaging allows the visualization and comparison of layers that are below the detection limit of the terahertz pulsed imaging instrument. On the other hand, it is expected that TPI is more suitable for very thick layers. As both methods are valuable tools to monitor the coating process, they may prove useful in a PAT context. They both have potential for rapid at-line analysis and process control. A very advantageous possibility could be the combination of both methods. TPI could be used for initial coating analysis, supported by NIR imaging where for example a higher spatial resolution is necessary. If a calibration of NIR imaging results at a specific wavelength with TPI results is successful, fast NIR measurements could be possible; this could lead to an on-line control of the coating process.

Acknowledgement

The authors would like to thank TeraView Ltd. for performing terahertz-measurements for selected samples.

References

Andersson, M., Josefson, M., Langkilde, F.W., Wahlund, K.-G., 1999. Monitoring of a film coating process for tablets using near infrared reflectance spectrometry. J. Pharm. Biomed. Anal. 20, 27–37.

Clarke, F., 2004. Extracting process-related information from pharmaceutical dosage forms using near infrared microscopy. Vib. Spectrosc. 34, 25–35.

Cogdill, R.P., Forcht, R.N., Shen, Y., Taday, P.F., Creekmore, J.R., Anderson, C.A., Drennen, J.K., 2007. Comparison of terahertz pulse imaging and near-infrared spectroscopy for rapid, non-destructive analysis of tablet coating thickness and uniformity. J. Pharm. Innov. 2, 29–36.

Day, G., Zeitler, J., Jones, W., Rades, T., Taday, P., 2006. Understanding the influence of polymorphism on phonon spectra: lattice dynamics calculations and terahertz spectroscopy of carbamazepine. J. Phys. Chem. B 110, 447–456.

El-Hagrasy, A.S., Morris, H.R., D'Amico, F., Lodder, R.A., Drennen, J.K., 2001. Near-infrared spectroscopy and imaging for the monitoring of powder blend homogeneity. J. Pharm. Sci. 90, 1298–1307.

El-Hagrasy, A.S., Chang, S.-Y., Desai, D., Kiang, S., 2006. Raman spectroscopy for the determination of coating uniformity of tablets: assessment of product quality and coating pan mixing efficiency during scale-up. J. Pharm. Innov. 1, 37–42.

FDA, 2004. Guidance for Industry: PAT—A Framework for Innovative Pharmaceutical Development, Manufacturing, and Quality Assurance.

Fitzgerald, A.J., Cole, B.E., Taday, P.F., 2005. Nondestructive analysis of tablet coating thicknesses using terahertz pulsed imaging. J. Pharm. Sci. 94, 177–183.

Gendrin, C., Roggo, Y., Collet, C., 2007. Content uniformity of pharmaceutical solid dosage forms by near infrared hyperspectral imaging: a feasibility study. Talanta 73, 733–741.

Ho, L., Muller, R., Romer, M., Gordon, K.C., Heinamaki, J., Kleinebudde, P., Pepper, M., Rades, T., Shen, Y.C., Strachan, C.J., Taday, P.F., Zeitler, J.A., 2007. Analysis of sustained-release tablet film coats using terahertz pulsed imaging. J. Control. Release 119, 253–261.

Kauffman, J.F., Dellibovi, M., Cunningham, C.R., 2007. Raman spectroscopy of coated pharmaceutical tablets and physical models for multivariate calibration to tablet coating thickness. J. Pharm. Biomed. Anal. 43, 39–48.

Kirsch, J.D., Drennen, J.K., 1995. Determination of film-coated tablet parameters by near-infrared spectroscopy. J. Pharm. Biomed. Anal. 13, 1273–1281.

Kirsch, J.D., Drennen, J.K., 1996. Near-infrared spectroscopic monitoring of the film coating process. Pharm. Res. 13, 234–237.

Lewis, E.N., Carroll, J.E., Clarke, F., 2001. A near infrared view of pharmaceutical formulation analysis. NIR News 12, 16–18.

Lyon, R.C., Lester, D.S., Lewis, E.N., Lee, E., Yu, L.X., Jefferson, E.H., Hussain, A.S., 2002. Near-infrared spectral imaging for quality assurance of pharmaceutical products: analysis of tablets to assess powder blend homogeneity. AAPS PharmSciTech 3 (article 17).

Malik, I., Poonacha, M., Moses, J., Lodder, R.A., 2001. Multispectral imaging of tablets in blister packaging. AAPS PharmSciTech 2 (article 9).

Mowery, M.D., Sing, R., Kirsch, J., Razaghi, A., Bechard, S., Reed, R.A., 2002. Rapid at-line analysis of coating thickness and uniformity on tablets using laser induced breakdown spectroscopy. J. Pharm. Biomed. Anal. 28, 935–943.

Pérez-Ramos, J.D., Findlay, W.P., Peck, G., Morris, K.R., 2005. Quantitative analysis of film coating in a pan coater based on in-line sensor measurements. AAPS PharmSciTech 6, E127–E136.

Reich, G., 2002. Potential of attenuated total reflection infrared and near-infrared spectroscopic imaging for quality assurance/quality control of solid pharmaceutical dosage forms. Pharm. Ind. 64, 870–874.

Roggo, Y., Jent, N., Edmond, A., Chalus, P., Ulmschneider, M., 2005. Characterizing process effects on pharmaceutical solid forms using near-infrared spectroscopy and infrared imaging. Eur. J. Pharm. Biopharm. 61, 100–110.

Romero-Torres, S., Perez-Ramos, J.D., Morris, K.R., Grant, E.R., 2005. Raman spectroscopic measurement of tablet-to-tablet coating variability. J. Pharm. Biomed. Anal. 38, 270–274.

Ruotsalainen, M., Heinamaki, J., Guo, H., Laitinen, N., Yliruusi, J., 2003. A novel technique for imaging film coating defects in the film-core interface and surface of coated tablets. Eur. J. Pharm. Biopharm. 56, 381–388.

Spencer, J.A., Gao, Z., Moore, T., Buhse, L.F., Taday, P.F., Newnham, D.A., Shen, Y., Portieri, A., Husain, A., 2007. Delayed release tablet dissolution related to coating thickness by terahertz pulsed image mapping. J. Pharm. Sci. 97, 1543–1550.

Wallace, V.P., Taday, P.F., Fitzgerald, A.J., Woodward, R.M., Cluff, J., Pye, R.J., Arnone, D.D., 2004. Terahertz pulsed imaging and spectroscopy for biomedical and pharmaceutical applications. Faraday Discuss. 126, 255–263 (discussion 303–311).

Walther, M., Fischer, B.M., Uhd Jepsen, P., 2003. Noncovalent intermolecular forces in polycrystalline and amorphous saccharides in the far infrared. Chem. Phys. 288, 261–268.

Zeitler, J.A., Shen, Y., Baker, C., Taday, P.F., Pepper, M., Rades, T., 2006. Analysis of coating structures and interfaces in solid oral dosage forms by three dimensional terahertz pulsed imaging. J. Pharm. Sci. 96, 330–340.